Structural determination of a molecular adsorbate by photoelectron diffraction: Ammonia on Ni{111}

K.-M. Schindler
Fritz-Haber-Institut der Max-Planck-Gesellschaft, Faradayweg 4-6, W-1000 Berlin 33, Germany

V. Fritzsche
Fritz-Haber-Institut der Max-Planck-Gesellschaft, Faradayweg 4-6, W-1000 Berlin 33, Germany
and Institut für Theoretische Physik, Technische Universität Dresden, Mommsenstrasse 13, O-8027 Dresden, Germany

M. C. Asensio
Instituto de Ciencia de Materiales, Consejo Superior de Investigaciones Científicas, Serrano 144, 28006 Madrid, Spain
and Physics Department, University of Warwick, Coventry CV4 7AL, United Kingdom

P. Gardner, D. E. Ricken, A. W. Robinson, and A. M. Bradshaw
Fritz-Haber-Institut der Max-Planck-Gesellschaft, Faradayweg 4-6, W-1000 Berlin 33, Germany

D. P. Woodruff
Physics Department, University of Warwick, Coventry CV4 7AL, United Kingdom

J. C. Conesa
Instituto de Catalysis y Petroleoquimica, Consejo Superior de Investigaciones Científicas, Serrano 119, 28006 Madrid, Spain

A. R. González-Elipe
Instituto de Ciencia de Materiales de Sevilla, Consejo Superior de Investigaciones Científicas, Apartado 1115, 41071 Sevilla, Spain
(Received 6 September 1991; revised manuscript received 5 March 1992)

The adsorption of ammonia (NH_3) on the Ni{111} surface has been investigated by photoelectron diffraction. To determine the adsorption site and the distance above the Ni{111} surface, photoelectron diffraction spectra of the N 1*s* core level were recorded in the scanned energy mode for normal and two off-normal emission directions and compared with extensive multiple-scattering calculations. The best agreement and the lowest *R* factor were found for an atop site and a Ni-N bond length of 1.97 Å. The anisotropic vibrations of the emitter have been taken into account in the theory and the mean-square displacement for the vibrations of the ammonia molecule parallel to the surface was determined to be 0.04 $Å^2$.

I. INTRODUCTION

Transition metals show very different activities when used as catalysts for the synthesis or decomposition of ammonia. Since the adsorption and desorption of the molecule itself are important steps in these reactions, a through characterization of the adsorbed ammonia molecule on these surfaces could lead to a better understanding of the differences. On the close-packed nickel {111} surface it is known that ammonia adsorbs molecularly with its threefold rotational axis normal to the surface.[1-8] The circular halo pattern obtained with electron stimulated desorption (ESDIAD) shows that the hydrogens point away from the surface and that the molecule is azimuthally either rotating or randomly oriented at 80 K.[1] Small amounts of preadsorbed oxygen change, however, the circular pattern into three spots, indicating an azimuthal locking as a result of hydrogen bonding to the oxygen atoms.[2] Angle-resolved photoemission spectroscopy has confirmed the upright geometry of the molecule by an analysis of the adsorbate-induced features using photoemission selection rules.[3] Using photoemission in an azimuthal angle-scan mode the same orientation of the hydrogens was found as with ESDIAD for the case of preadsorbed oxygen; the azimuthal ordering was therefore interpreted as being due to small amounts of surface contaminants.[4] Long-range-ordered structures have not yet been unambiguously identified because of the difficulties involved in making precise low-energy electron diffraction (LEED) measurements. It is well established that NH_3 decomposes on the Ni{111} surface under electron bombardment,[1,3,5] giving rise eventually to a clear (2×2) pattern which has been tentatively assigned to adsorbed NH_x $(x=1,2)$.[3] With a special low current LEED system a weak $(\sqrt{7}\times\sqrt{7})R19°$ pattern was found over a wide range of coverage and temperature.[5] The sensitivity to incident electrons makes it difficult to determine the exact adsorption geometry by recording LEED *I-V* curves and making subsequent comparison with dynamical calculations.

From temperature-programmed desorption (TPD) it is known that below 90 K ammonia multilayers are formed,

 ©1992 The American Physical Society

which desorb as a sharp peak at ~120 K.[1,2(b),3,5,6,8] The remaining monolayer then desorbs as molecular NH_3 over a wide range up to 350 K. Thermal decomposition to NH_x ($x=1,2$) and atomic nitrogen were detected only in traces and might well be due to the presence of surface defects. The coverage of the ammonia monolayer (saturation coverage) has been given as 0.25 [Ref. 2(b)] and 1.0.[3] The latter value was corrected to <0.3 in a subsequent paper;[4] a further value of 0.14 was derived after a reinterpretation of the TPD and LEED measurements.[6]

The bonding and structure of the Ni{111}-NH_3 system has also been studied by means of quantum-chemical calculations. Recent *ab initio* valence-orbital configuration-interaction calculations[9] for an ammonia molecule on a 28-atom nickel cluster gave the lowest total energy for the atop site with a Ni-N bond length of 2.12 Å. The differences in total energy between the atop site, the fcc threefold hollow site (underlying nickel atom in the third layer), and the bridge site were small, however. The Ni-N bond lengths resulting from the calculations for the latter two positions were unexpectedly large (2.78 and 2.74 Å, respectively). The equilibrium geometry was calculated to have the molecular axis perpendicular to the surface, but tilting the molecular axis or rotating the molecule azimuthally requires little energy. In an earlier study at the Hartree-Fock level, in which only the fcc threefold hollow site was considered, the Ni-N bond length was given as 2.13 Å.[10]

In the present paper we have used scanned energy mode photoelectron diffraction to determine the structure of NH_3 on Ni{111}. This technique involves the measurement of the intensity of photoelectrons emitted from a core level of the adsorbate in a selected direction as a function of photon energy and thus of the kinetic energy of the photoelectron. In the plot of intensity versus kinetic energy ("the photoelectron diffraction spectrum") modulations can be seen as a result of interference of the primary photoelectron wave and secondary waves elastically scattered at surrounding atoms. The form of the intensity modulations is determined by the distance and directions of the neighboring atoms and hence carries the desired structural information. Due to its local character the effect is not dependent on the presence of long-range order. Energy-scan photoelectron diffraction has already been shown to be a useful tool for the determination of adsorption sites and bond lengths for a number of other atomic and molecular adsorption systems.[11]

II. EXPERIMENT

The UHV system for the experiments is equipped with a four-grid LEED optics, a quadrupole mass spectrometer, a gun for ion bombardment, and a hemispherical electron analyzer (ADES 400, VG Scientific Ltd). The temperature of the sample could be varied between 100 and 1000 K by LN_2 cooling and resistive heating through tungsten wires which held the crystal in position. The temperature of the sample was measured by a thermocouple in direct contact with the crystal. The surface of a nickel crystal was prepared in the usual way, including *in situ* argon ion bombardment and annealing cycles up to 800 K until a well-ordered (1×1) LEED pattern was obtained and x-ray photoemission spectra (XPS) measurements with synchrotron radiation revealed no surface contamination. The LEED pattern was also used to determine the azimuthal orientation of the crystal. Ammonia was used as purchased (Linde AG, 99.98%). Saturation coverage of ammonia was achieved by an exposure of 40 sec at 5×10^{-7} mbar with the sample at ~ 110 K. The purity of the adsorbed layer was checked with XPS. Special attention was paid to carbon- and oxygen-containing contaminations.

Measurements were performed using synchrotron radiation from the high-energy toroidal grating monochromator HE-TGM 1 on the Berliner Elektronen Speicherring-Gesellschaft für Synchrotron-Strahlung electron storage ring.[12] The general method of taking scanned energy mode photoelectron diffraction data has been explained in previous publications[11,13] but is also described here since some of the details have now changed.

Figure 1 shows a series of normalized N 1*s* photoelectron spectra for NH_3 adsorbed on the Ni(111) surface at saturation coverage and a sample temperature of ~100 K. The electric vector of the incident radiation lies in the plane spanned by the surface normal and the [1$\bar{1}$0] azimuth, which is the direction of the close-packed nickel atom rows, (see also inset of Fig. 1) at an angle of 45° to the surface normal. The photon energy of the incident radiation was varied from 490 to 750 eV in steps of 3.5 eV. The corresponding binding energy of the N 1*s* core level then leads to kinetic energies of the photoelectrons in the range from 90 to 350 eV. For each photon energy a photoelectron spectrum was recorded in a window of kinetic electron energy with the N 1*s* peak near the center of the spectrum and a width of 50 eV; for the sake of clarity only every second spectrum recorded is shown in Fig. 1. These spectra were normalized to the current in the electron storage ring to correct the decrease in photon flux with time. Since the width of the N 1*s* pho-

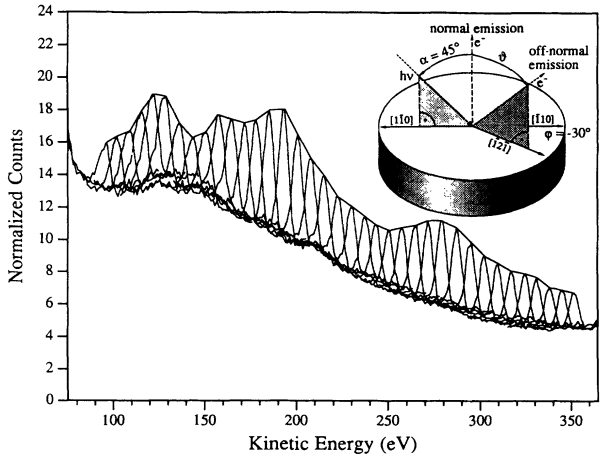

FIG. 1. Experimental N 1*s* photoelectron spectra of NH_3 on the Ni{111} surface in normal emission for a series of incident photon energies. Only every second spectrum is shown. Inset: experimental geometry.

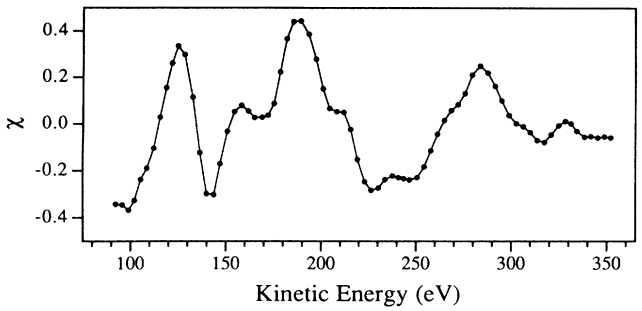

FIG. 2. Experimental photoelectron diffraction spectrum of NH_3 on the Ni{111} in the normal emission direction obtained by analysis of the individual spectra in Fig. 1.

toelectron peak is a smoothly varying function and the background is also relatively smooth, the outline formed by the peak maxima already shows the modulations of the N 1*s* peak intensity. To obtain the N 1*s* photoelectron peak areas the spectra were fitted simultaneously with an asymmetric Gaussian for the peak and a polynomial of third order for the background using a standard nonlinear least-square-fitting-routine. To obtain the photoelectric intensity $I(E_{\rm kin})$ the integral of the Gaussian was calculated from its height and width. Plotting the intensities of all peaks versus the kinetic energies of their maxima then gave the raw photoelectron diffraction spectrum.

In order to correct for the smoothly varying transmission functions of the monochromator and the analyzer a least-square fit by a polynomial of third order is performed on the raw photoelectron diffraction spectrum. This polynomial represents $I_0(E_{\rm kin})$, the intensity without scattering processes. The photoelectron diffraction data can then be represented in the form of a modulation function χ,

$$\chi(E_{\rm kin})=\frac{I(E_{\rm kin})-I_0(E_{\rm kin})}{I_0(E_{\rm kin})} , \tag{1}$$

which oscillates about zero. The $\chi(E_{\rm kin})$ obtained from the raw data in Fig. 1 is shown in Fig. 2. The modulations in photoelectron intensity due to the diffraction processes are $\sim\pm 40\%$. During the analysis it was found that the subtraction of the background polynomial in each N 1*s* photoelectron spectrum is a source of error and could give rise to an uncertainty of $\pm 5\%$ in $\chi(E_{\rm kin})$. Three maxima at 125, 190, and 280 eV and two minima at 140 and 225 eV are the most significant features in the spectrum of Fig. 2. The minimum at 100 eV may not be significant, because the error introduced by the data analysis becomes larger at this end of the spectrum.

III. THEORY

Proper quantitative determination of the structure of NH_3 on Ni{111} from the photoelectron diffraction spectra requires the use of extensive multiple-scattering cluster calculations. Within a first-order perturbation theory the intensity of the outgoing photoelectron signal is given by

$$I(\mathbf{r})\sim \left| \int d^3r' G(\mathbf{r},\mathbf{r}';E_f)\,\mathbf{A}\cdot\mathbf{p}\Psi_c(\mathbf{r}') \right|^2 , \tag{2}$$

where $\mathbf{A}$ is the vector potential of the photon field, $\mathbf{p}$ the momentum operator of the electrons, Ψ_c the core orbital which is excited, and $\mathbf{r}$ the detector position. The Green function of the total system $G(\mathbf{r},\mathbf{r}';E_f)$, which has to be taken at the final-state energy E_f, can be expanded into a series over all possible pathways which connect the emitter via scattering centers to the detector.[14,15] The wave-function contributions from these hypothetical scattering pathways have been calculated on the basis of a magnetic-quantum-number expansion described in Refs. 16 and 17. In this method an optimized set of basis functions is used for the angular-momentum representation in the scattering theory. As a consequence, all sums over magnetic quantum numbers converge rapidly and can be truncated after a few terms without any loss of accuracy.[18,19] The essential terms in this scheme are rotation matrices which determine the optimum linear combination of basis functions for each scattering process and *z*-axis propagators in two center angular momentum representation. Both matrices have been calculated by means of fast recursion relations given in Ref. 20.

The essential difference compared to other approaches which are used for multiple-scattering cluster simulation of photoelectron diffraction spectra is that the matrix elements of the free-electron propagator are calculated without any approximation. Recently, it has been shown[19] that the principle of "separable approximations" for the free-electron Green function, in which the angular momentum indices l and l' of the *z*-axis propagators are decoupled in order to save computer time, can be the origin of substantial errors for the case that both l and l' have large values. Hence, the Taylor-series magnetic-quantum-number expansion,[17] the reduced angular momentum expansion,[16] and the scattering matrix formulation,[21] which all belong to this class of approximations, can introduce considerable uncertainty into the results for all second- and higher-order scattering processes, if the distance between emitter and scatterer is small (nearest neighbors), i.e., for all scattering processes of a scattered wave which contains the full set of partial waves (see Ref. 19 for more details).

In the present calculations the truncation parameter in the magnetic-quantum-number expansion[20] was set to $M=3$ for all emitter-scatterer distances R shorter than 4 Å, $M=2$ for $R\leq 10$ Å, and $M=1$ otherwise. The calculations were performed with up to 18 scattering phase shifts for nickel potentials at the highest energy. The effect of inelastic scattering processes was described by exponential damping factors containing the mean free path of electrons for which the "universal" values from Seah and Dench were assumed.[22]

The finite energy resolution, a fundamental property of the experiment, was taken into account from the outset. This energy broadening of a photoelectron diffraction spectrum leads to additional damping factors in the theoretical expression for the intensity which systematically suppress the contributions of long scattering path-

ways.[23] Thus, the calculation of a smoothed scanned energy mode photoelectron diffraction spectrum requires considerably less numerical effort than the correct calculation of an unbroadened spectrum, because a smaller set of scattering pathways is sufficient for convergence and a larger separation between two grid points on the energy scale can be chosen.

The theoretical calculations shown below contain the contributions of ~1000 single scattering and ~5000 double scattering processes. It turned out that the double scattering processes, which require most of the computing time, give noticeable contributions to the intensity and therefore cannot be neglected. In the present example triple- and higher-order scattering pathways could be neglected, because they are damped out by the energy broadening due to their larger scattering path lengths. This was checked by test calculations at selected energies.

IV. DETERMINATION OF THE ADSORPTION SITE AND THE NI-N BOND LENGTH

Strong modulations in energy-scan photoelectron diffraction spectra are normally indicative of a dominant contribution from one scattering pathway. This often corresponds to a particular geometry in which a substrate atom is directly "behind" the emitting atom, i.e., when emitter, scatterer, and detector are colinear. In such a configuration the strong 180° backscattering expected for $E_{kin} < 500$ eV dominates. From the normal emission spectrum of Fig. 2 we might therefore expect that the molecule occupies an atop site, although there is also the possibility, perhaps less likely, that the hcp threefold hollow site is occupied. (This latter site has an underlying nickel atom in the second layer, as opposed to the fcc threefold hollow site where the underlying nickel atom is in the third layer.) In the simulations, however, all four high-symmetry sites, including the twofold bridge and the fcc threefold hollow, have been considered.

Scattering processes at hydrogen atoms were neglected since their scattering cross sections are very much smaller than those of the substrate atoms. Furthermore, there is a strong evidence from theory and experiment that the hydrogen atoms are rotating or randomly oriented azimuthally on the clean surface,[19] which additionally decreases their contributions to the intensity modulations. The neglect of the hydrogens thus reduces the ammonia molecule to a single nitrogen atom. Scattering contributions of neighboring nitrogen atoms were also neglected since their relative positions are not known. On the assumption that the coverage is below 0.5, the distance from the emitting nitrogen atom to the nearest nitrogen atoms will be larger than the distances to the substrate atoms which dominate the backscattering. Furthermore, the scattering cross section of the nitrogen atom is much smaller than that of the nickel atoms.

Figure 3 shows the calculated photoelectron diffraction spectra for a series of separations between the nitrogen atom and the outermost Ni layer, z, at each of the four high-symmetry sites. For comparison the experimental diffraction spectrum has been included as a dashed curve in each plot. By comparing the calculated and the experimental curves, the best agreement regarding the positions and relative heights of the maxima and minima is found for the atop site with a Ni-N bond length of 1.975 Å [Fig. 3(a)]. Reasonable agreement is also found for the fcc threefold hollow site at $z = 1.3$ Å [Fig. 3(c)]. Even as far as the absolute amplitudes are concerned, the agreement for the atop site is remarkably good. The twofold bridge [Fig. 3(b)] and the hcp threefold hollow [Fig. 3(d)] do not give agreement for any distance.

The experimental and calculated spectra have also been compared by means of the reliability factor R_p,[24] although it is not entirely clear whether R factors developed for LEED are appropriate for photoelectron diffraction. Such an R-factor plot for the atop site shows a clear minimum of 0.32 at 1.97 Å, as shown in Fig. 4. It is difficult to give a definite value for the precision of the determination. We note that even by visible inspection agreement between theory and experiment is not as good for 2.00 and 1.95 Å and considerably worse for 2.025 and 1.925 Å. A value of ±(0.02–0.03) Å would therefore seem plausible, in line with other photoelectrons diffraction studies.[25] However, as in LEED, there is also the possibility of systematic errors arising from the

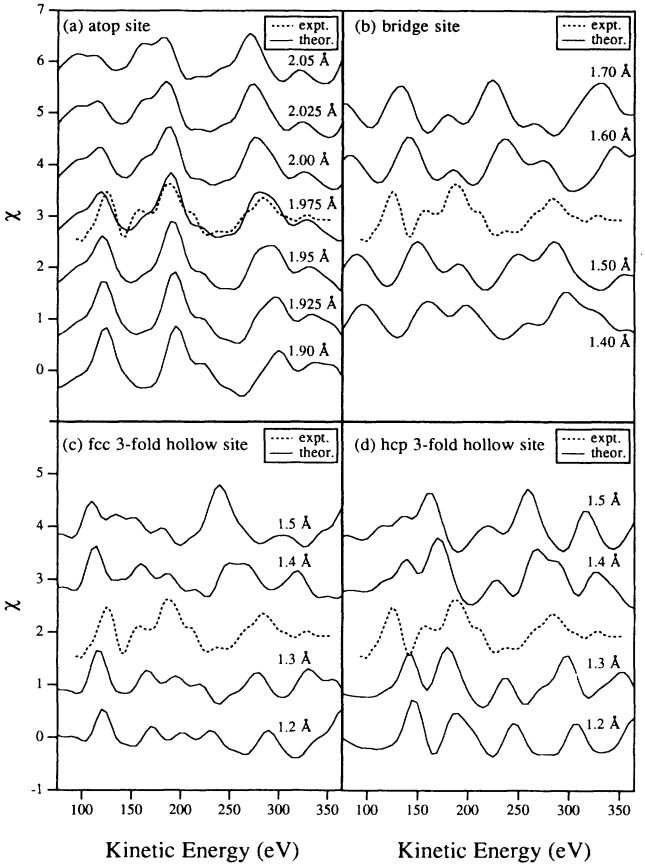

FIG. 3. Calculated photoelectron diffraction spectra for NH_3 on Ni{111} in normal emission for (a) the atop, (b) the bridge, (c) the fcc threefold hallow, and (d) hcp threefold hollow sites for various separations between the N atom and the outermost nickel layer. For the sake of clarity the spectra are offset against each other by unity on the vertical axis.

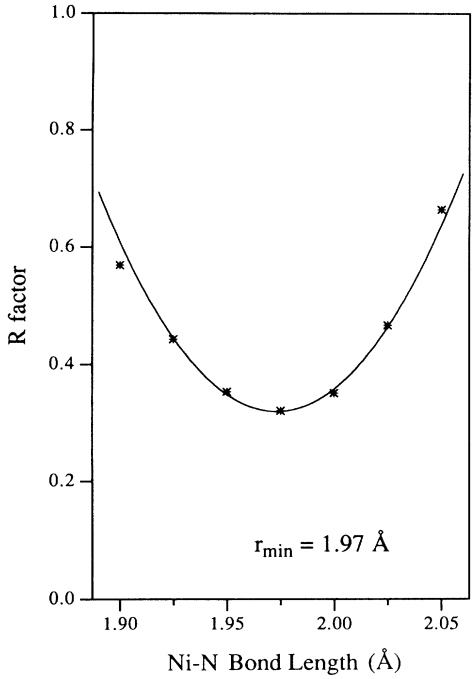

FIG. 4. Reliability factors R_p for the atop-site spectra shown in 3(a).

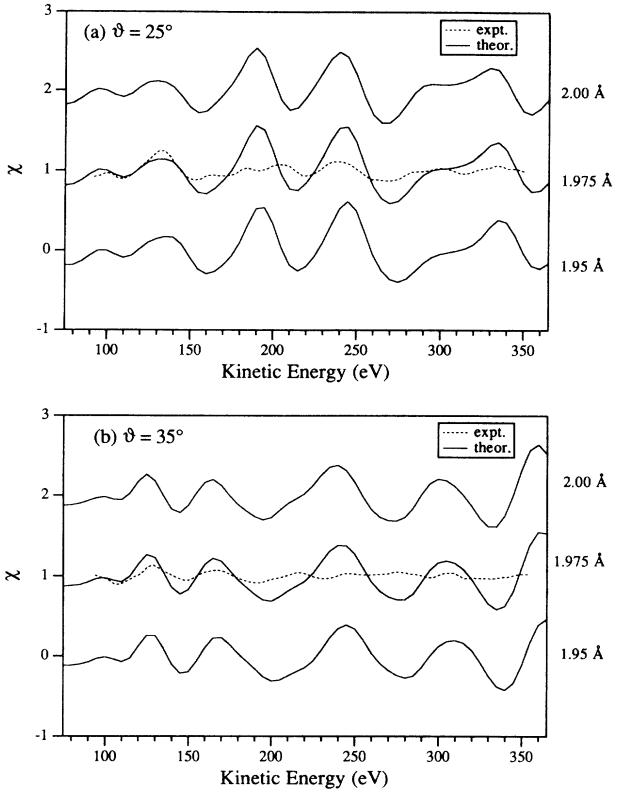

FIG. 5. Comparison of calculated and measured off-normal photoelectron diffraction spectra for the atop site without taking into account adsorbate vibrations. Polar angle ϑ in the $[\bar{1}2\bar{1}]$ azimuth: (a) 25°, (b) 35°.

theory. Test calculations on the present system have, for instance, shown that the uncertainty as to the potential in the surface region can give rise to an error as high as ±0.05 Å. The fcc threefold hollow site gives a shallow R-factor minimum of 0.56 at 1.30 Å; the hcp threefold hollow site and the bridge site give $R_p > 1.0$ and no minimum.

Although the comparison of experimental and calculated diffraction spectra in normal emission clearly favors the atop site, it is desirable to check the structure with measurements in off-normal emission directions. However, it was found experimentally that in all directions the intensity modulations were much smaller than in normal emission. Thus, for the two polar angles $\vartheta = 25°$ and 35° in the $[\bar{1}2\bar{1}]$ azimuth, as shown in Fig. 5, the modulations were less than ±15%, which is already quite close to the discrepancy between experimental and calculated spectra in normal emission of about 5%. Therefore, worse agreement between theory and experimental as well as higher R factors than in normal emission are expected. As the modulations are so small, it was also necessary to correct for the Ni Auger peak at a kinetic energy of ~105 eV.

A comparison of the experimental and calculated spectra in off-normal emission shows some, but not particularly good agreement regarding the positions of maxima and minima for the atop site (Fig. 5). The corresponding R factors have very shallow minima with values 0.63 ($\theta = 25°$) and 0.78 ($\theta = 35°$) for the atop site and a Ni-N distance of 1.975 Å. Some agreement was also found for the hcp threefold hollow, but this site was convincingly ruled out on the basis of the normal emission spectrum. Complete disagreement was observed for the bridge site and, more important, for the fcc threefold hollow site. Although the agreement is far from satisfactory and the R factors are high, the off-normal spectra confirm the assignment based on the normal emission spectrum. Particularly striking, however, is the fact that the modulation amplitude in the calculated spectra is a factor of 2–3 larger than in the experimental spectra, i.e., comparable to that calculated and observed in normal emission. We ascribe this effect to the influence of adsorbate vibrations and discuss it in Sec. V.

V. ANISOTROPIC THERMAL VIBRATIONS OF THE EMITTER

The large difference in absolute amplitude between experiment and theory for off-normal emission can be explained by damping due to the soft vibrational modes of the ammonia molecule parallel to the surface, the frustrated translations and rotations.[26] This assumption is supported by quantum-chemical calculations,[9] in which it was found that a tilt of ammonia up to 10° requires only very little energy, indicating a shallow total-energy surface for soft modes parallel to the surface. The latter are expected to be considerably softer than the vibration of the molecule against the surface (the Ni-N stretch) as can be seen from the good agreement in the modulation amplitude of the calculated and measured spectra in normal emission. The influence of this parallel vibrational motion on the off-normal emission spectra should be much larger than on the normal emission spectrum, since

the changes in scattering path lengths are much less in the latter case. These frustrated translations and rotations which give rise to the parallel motion of the emitter can be included in the calculation scheme as follows:

The wave function of the excited electrons is given as a sum over all scattering pathways, which start at the emitter atom and terminate at the detector outside the sample. We thus have

$$\Psi=\sum_{\alpha}\varphi_{\alpha}\ , \tag{3}$$

where the sum runs over all relevant scattering pathways. The wave field components φ_{α} depend on the positions of the emitter $\mathbf{R}_0$, the scattering atoms $\mathbf{R}_i$, and the detector $\mathbf{r}$,

$$\varphi_{\alpha}=\varphi_{\alpha}(\mathbf{R}_1-\mathbf{R}_0,\mathbf{R}_2-\mathbf{R}_1,\cdots,\mathbf{r}-\mathbf{R}_n)\ . \tag{4}$$

These vectors $\mathbf{R}_i$ can be split into an equilibrium value $\langle\mathbf{R}_i\rangle$ and a displacement $\mathbf{u}_i$, which describes the thermal motions of the atoms,

$$\mathbf{R}_i=\langle\mathbf{R}_i\rangle+\mathbf{u}_i\ . \tag{5}$$

For small displacements we can write the phase in the propagators between two positions as

$$k|\mathbf{R}_j-\mathbf{R}_i|\approx k|\langle\mathbf{R}_j\rangle-\langle\mathbf{R}_i\rangle|+\mathbf{K}_{ji}\cdot(\mathbf{u}_j-\mathbf{u}_i) \tag{6}$$

with

$$\mathbf{K}_{ji}=k\frac{\langle\mathbf{R}_j\rangle-\langle\mathbf{R}_i\rangle}{|\langle\mathbf{R}_j\rangle-\langle\mathbf{R}_i\rangle|}\ ,$$

where k is the wave number of the electron. Thus the essential influence of thermal vibrations on the electron wave function is concentrated in a phase factor, which is multiplied by the wave function corresponding to the equilibrium position:

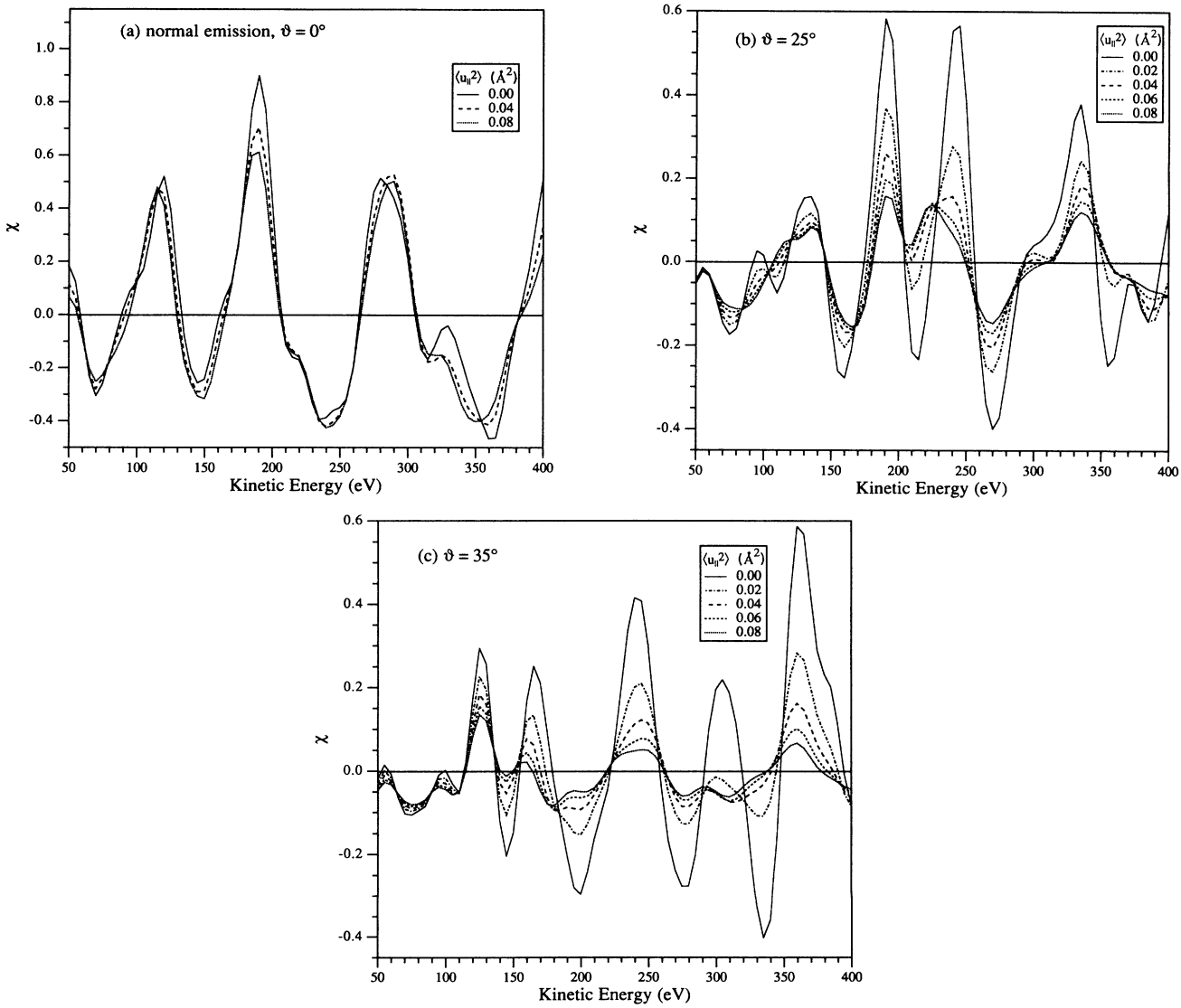

FIG. 6. Calculated photoelectron diffraction spectra of atop NH_3 on Ni(111) in (a) normal and two off-normal emission directions. Polar angle ϑ in the $[\bar{1}2\bar{1}]$ azimuth: (b) 25°, (c) 35°. Vibrational motions of the emitting nitrogen atom parallel to the surface are included by means of a mean-square displacement $\langle u_{\parallel}^2\rangle$ as indicated in the diagram.

$$\varphi_\alpha(\mathbf{R}_1-\mathbf{R}_0,\mathbf{R}_2-\mathbf{R}_1,\cdots,\mathbf{r}-\mathbf{R}_n)=\exp[i\mathbf{K}_{10}\cdot(\mathbf{u}_1-\mathbf{u}_0)+i\mathbf{K}_{21}\cdot(\mathbf{u}_2-\mathbf{u}_1)+\cdots]$$
$$\times\varphi_\alpha(\langle\mathbf{R}_1\rangle-\langle\mathbf{R}_0\rangle,\langle\mathbf{R}_2\rangle-\langle\mathbf{R}_1\rangle,\cdots,\mathbf{r}-\langle\mathbf{R}_n\rangle)\,. \quad (7)$$

Assuming an uncorrelated motion of the atoms the averaging procedure over the various displacements $\mathbf{u}_i$ in the intensity

$$I=\left\langle\left|\sum_\alpha\varphi_\alpha\right|^2\right\rangle \quad (8a)$$

$$=\left\langle\sum_{\alpha,\alpha'}\varphi^*_{\alpha'}\varphi_\alpha\right\rangle \quad (8b)$$

can be decoupled and the vibrations of each atom can be treated separately. In our calculations the effect of the motion of the scattering atoms was described by complex scattering phase shifts.[27] The same result can be obtained by using Debye-Waller factors for the scattering atoms (see, e.g., Refs. 28 and 29). However, at a temperature of $\sim$110 K at which the experiment was performed, the influence of lattice vibrations in the nickel crystal on the photoelectron diffraction spectra is very small. Vibrations of the adsorbate molecule are more important, since they can have considerably larger amplitudes, particularly parallel to the surface. These effects, which have been neglected in the past, are not automatically described by complex scattering phase shifts. Hence, we have to introduce an additional Debye-Waller factor in the expression for the intensity, which contains the result of the averaging over the emitter displacements $\mathbf{u}_0$.

In the formula for the intensity (8b) $\mathbf{u}_0$ appears both in the φ_α and in $\varphi^*_{\alpha'}$. Using standard techniques for describing harmonic vibrations[30] we obtain for the Debye-Waller term in the double sum (8b):

$$\left\langle\exp[i(\mathbf{K}'_{10}-\mathbf{K}_{10})\cdot\mathbf{u}_0]\right\rangle$$
$$=\exp\left[-\tfrac{1}{2}(\mathbf{K}'_{10}-\mathbf{K}_{10})\cdot\langle\mathbf{u}_0\cdot\mathbf{u}_0\rangle\cdot(\mathbf{K}'_{10}-\mathbf{K}_{10})\right]\,, \quad (9)$$

where $\mathbf{K}_{10}$ points in the direction of the first scattering atom $\mathbf{R}_1$ in the scattering pathway with index α and K'_{10} is the same vector in the scattering pathway with index α'. In Eq. (9) the influence of the vibrations is described by the tensor $\langle\mathbf{u}_0\cdot\mathbf{u}_0\rangle$. For isotropic vibrations it is diagonal with $\langle u_x^2\rangle=\langle u_y^2\rangle=\langle u_z^2\rangle$. As mentioned above, for adsorbate atoms or molecules on a surface highly anisotropic displacements can be expected, for which the components parallel to the surface $\langle u_x^2\rangle=\langle u_y^2\rangle=\langle u_\parallel^2\rangle$ differ significantly from the component perpendicular to the surface $\langle u_z^2\rangle=\langle u_\perp^2\rangle$.

Figure 6 shows the calculated diffraction spectra for all three measured emission directions. Calculations were performed for different values of $\langle u_\parallel^2\rangle$, assuming that the molecule does not vibrate perpendicular to the surface ($\langle u_\perp^2\rangle=0$). The plots show that the off-normal spectra can be influenced dramatically by parallel vibrations. As a general trend it is observed that the damping effect is more pronounced at higher energies due to the k dependence of the Debye-Waller factor [Eq. (9)]. The main change is in absolute magnitude. Some peaks are influenced more strongly than others which then also leads to changes in the positions of some extremal points, for example, the maximum at 240 eV for $\vartheta=25°$. In the spectrum for $\vartheta=35°$ the minimum at 200 eV and the maximum at 300 eV even vanish with increasing mean-square displacements. The changes in the normal emission spectrum, however, are only minor and, more important, the peak positions hardly change.

Best agreement between experiment and theory for both off-normal emission directions was found for $\langle u_\parallel^2\rangle=0.04$ Å^2, which is reflected by a decrease of the R factor from 0.63 to 0.50 ($\theta=25°$) and from 0.78 to 0.43 ($\theta=35°$). A mean-square displacement of 0.04 Å^2 corresponds to an average dynamic tilt of the molecular axis of 6°, a value which is well within the error bars of the

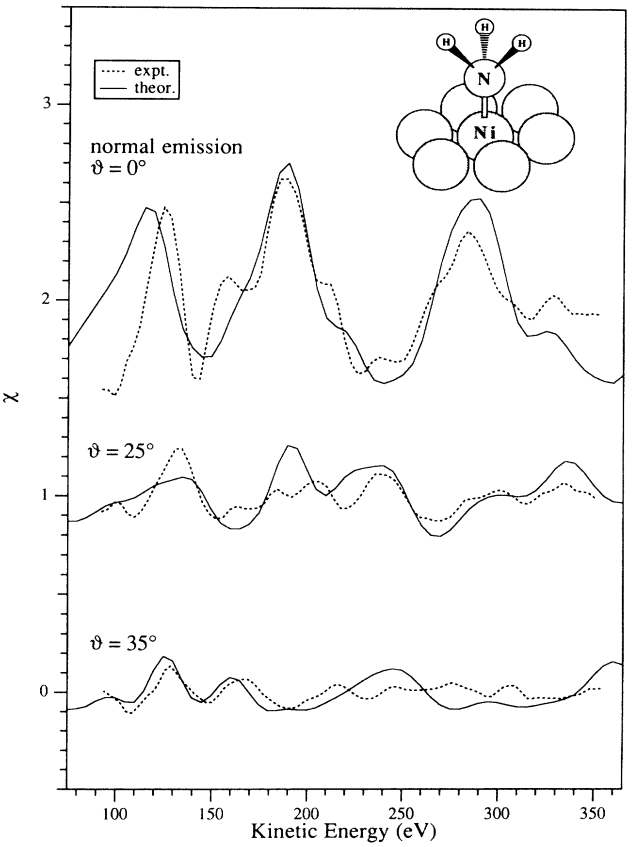

FIG. 7. Comparison of experimental photoelectron diffraction spectra with calculated spectra in the three emission directions recorded. Calculations are performed for the atop site with Ni-N bond length of 1.975 Å and a mean-square displacement of the nitrogen parallel to the surface $\langle u_\parallel^2\rangle$ of 0.04 Å^2.

orientation determination using angle-resolved photoemission and ESDIAD. Figure 7 shows the comparison of calculated and experimental photoelectron diffraction spectra for all three emission directions after including the influence of the anisotropic vibrations of the emitter.

VI. CONCLUSIONS

Scanned energy mode photoelectron diffraction has been successfully applied to ammonia adsorbed on Ni{111}. The adsorption site and the Ni-N bond length could be determined by comparing experimental and calculated photoelectron diffraction spectra. The structure of the adsorption complex with NH_3 in the atop site is schematically shown in the inset of Fig. 7. With the lone pair of the nitrogen atom directed towards one nickel atom, the structure resembles the usual sp^3 fourfold coordination expected for nitrogen. The Ni-N bond length of 1.97 Å compares well with that of nickel ammine complexes such as $Ni(NO_2)_2(NH_3)_4$ with 2.07 Å (Ref. 31) or ammine[1-(2-hydroxyphenyl)-3, 5-diphenylformazanato]nickel(II) with 1.94 Å.[32] It has also been shown that the anisotropic vibrational motion of the emitter atom must be considered in order to describe correctly the amplitude of the modulations in the diffraction spectra at off-normal emission. The mean-square displacement of the molecule parallel to the surface $\langle u_{\parallel}^2 \rangle$ was estimated to be 0.04 Å^2.

ACKNOWLEDGMENTS

We acknowledge financial support from the German Federal Ministry of Research and Technology (Contract No. 05-490-FXB8.4), the Fonds der Chemischen Industrie, the Science and Engineering Research Council (United Kingdom) as well as the Large Installations and the SCIENCE programmes of the European Commission.

[1]T. E. Madey, J. E. Houston, C. W. Seabury, and T. N. Rhodin, J. Vacuum Sci. Technol. **18**, 476 (1981).

[2](a) F. P. Netzer and T. E. Madey, Phys. Rev. Lett. **47**, 928 (1981); (b) Surf. Sci. **119**, 422 (1982).

[3]C. W. Seabury, T. N. Rhodin, R. J. Purtell, and R. P. Merrill, Surf. Sci. **93**, 117 (1980).

[4]W. M. Kang, C. H. Li, S. Y. Tong, C. W. Seabury, K. Jacobi, T. N. Rhodin, R. J. Purtell, and R. P. Merrill, Phys. Rev. Lett. **47**, 931 (1981).

[5]C. W. Seabury, T. N. Rhodin, R. J. Purtell, and R. P. Merrill, J. Vacuum Sci. Technol. **18**, 602 (1981).

[6]M. J. Dresser, A-M Lanzillotto, M. D. Alvey, J. T. Yates, Jr., Surf. Sci. **191**, 1 (1987).

[7]F. Bozso, J. M. Arias, C. P. Hanrahan, J. T. Yates, Jr., H. Metiu, and R. M. Martin, Surf. Sci. **138**, 488 (1984).

[8]G. B. Fisher and G. E. Mitchell, J. Electron Spectrosc. Relat. Phenom. **29**, 253 (1989).

[9]A. Chattopadhyay, H. Yang, and J. L. Whitten, J. Phys. Chem. **94**, 6379 (1990).

[10]A. Redondo, Y. Zeiri, J. J. Low, and W. A. Goddard, J. Chem. Phys. **79**, 6410 (1983).

[11]J. J. Barton, S. W. Robey, and D. A. Shirley, Phys. Rev. B **34**, 778 (1986); S. W. Robey, C. C. Bahr, Z. Hussain, J. J. Barton, K. T. Leung, Ji-rin Lou, R. A. Schach von Wittenau, and D. A. Shirley, Phys. Rev. B **35**, 5657 (1987); M. D. Crapper, C. E. Riley, P. J. J. Sweeney, C. F. McConville, D. P. Woodruff, and R. G. Jones, Surf. Sci. **182**, 213 (1987); D. P. Woodruff, C. F. McConville, A. L. D. Kilcoyne, Th. Lindner, J. Somers, M. Surman, G. Paolucci, and A. M. Bradshaw, Surf. Sci. **201**, 228 (1988).

[12]E. Dietz, W. Braun, A. M. Bradshaw, and R. L. Johnson, Nucl. Instrum. Methods A **239**, 359 (1985).

[13]Th. Lindner, J. Somers, A. M. Bradshaw, A. L. D. Kilcoyne, and D. P. Woodruff, Surf. Sci. **203**, 333 (1988).

[14]A. Liebsch, Phys. Rev. B **13**, 544 (1976).

[15]T. Fujikawa, J. Electron Spectrosc. **22**, 353 (1981).

[16](a) V. Fritzsche and P. Rennert, in *Proceedings of the 14th Symposium on Electronic Structure,* edited by P. Ziesche, Dresden (Technische Universität, Dresden, 1984), p. 77. (b) V. Fritzsche and P. Rennert, Phys. Status Solidi B **135**, 49 (1986).

[17](a) J. J. Barton and D. A. Shirley, Phys. Rev. B **32**, 1906 (1985). (b) J. J. Barton and D. A. Shirley, Phys. Rev. A **32**, 1019 (1985).

[18]V. Fritzsche, J. Phys.: Condens. Matter **2**, 1413 (1990).

[19]V. Fritzsche, J. Electron Spectrosc. **58**, 299 (1992).

[20]V. Fritzsche, J. Phys.: Condens. Matter **2**, 9735 (1990).

[21]J. J. Rehr and R. C. Albers, Phys. Rev. B **41**, 8139 (1990); A. P. Kaduwela, D. J. Friedman, and C. S. Fadley, J. Electron. Spectrosc. **57**, 223 (1991).

[22]M. P. Seah and W. A. Dench, Surf. Interface Anal. **1**, 2 (1979).

[23]V. Fritzsche, Surf. Sci. **265**, 187 (1992).

[24]J. B. Pendry, J. Phys. C **13**, 937 (1980).

[25]L. J. Terminello, X. S. Zhang, Z. Q. Huang, S. Kim, A. E. Schach von Wittenau, K. T. Leung, and D. A. Shirley, Phys. Rev. B **38**, 3879 (1988).

[26]N. V. Richardson and A. M. Bradshaw, Surf. Sci. **88**, 255 (1979).

[27]J. B. Pendry, *Low Energy Electron Diffraction* (Academic, London, 1974).

[28]J. J. Barton, S. W. Robey, and D. A. Shirley, Phys. Rev. B **34**, 778 (1986).

[29]M. Sagurton, E. L. Bullock, and C. S. Fadley, Surf. Sci. **182**, 287 (1987).

[30]A. A. Maradudin, E. W. Montroll, G. H. Weiss, and I. P. Ipatova, *Theory of Lattice Dynamics in the Harmonic Approximation,* Solid State Physics Supplement 3 (Academic, New York, 1971), Chap. VII, pp. 300.

[31]M. A. Paraj-Kojic, A. S. Antzishkina, L. M. Dickareva, and E. K. Jukhnov, Acta Crystallogr. **10**, 784 (1957).

[32]W. E. Renkema, C. N. Lute, and C. H. Stam, Acta Crystallogr. Sect. B **35**, 75 (1979).

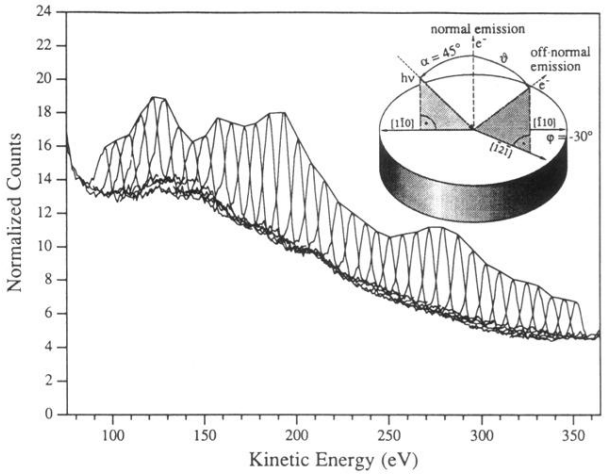

FIG. 1. Experimental N 1*s* photoelectron spectra of NH_3 on the Ni{111} surface in normal emission for a series of incident photon energies. Only every second spectrum is shown. Inset: experimental geometry.

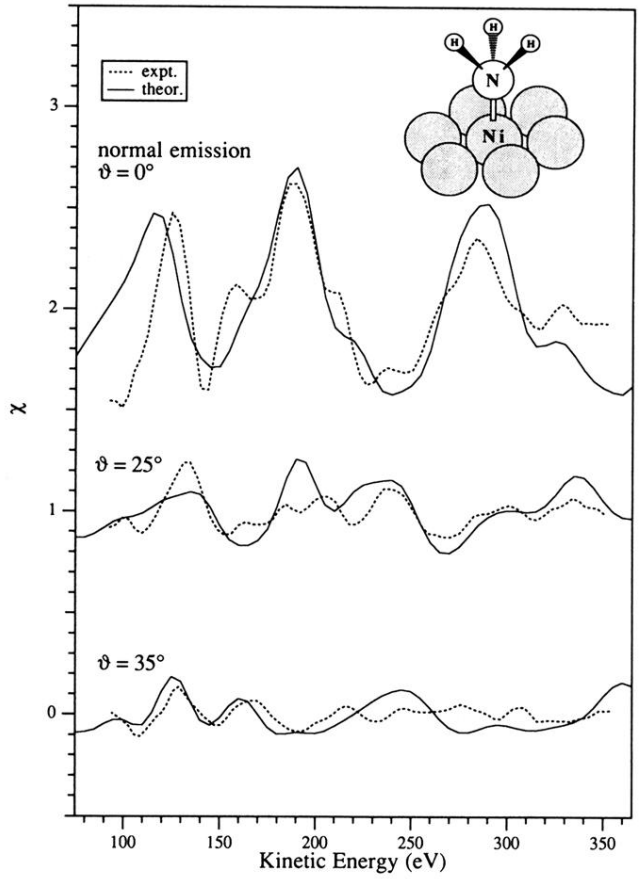

FIG. 7. Comparison of experimental photoelectron diffraction spectra with calculated spectra in the three emission directions recorded. Calculations are performed for the atop site with Ni-N bond length of 1.975 Å and a mean-square displacement of the nitrogen parallel to the surface $\langle u_{\parallel}^2 \rangle$ of 0.04 Å^2.